

Insights into the adsorption of water and oxygen on the cubic $CsPbBr_3$ surfaces: A first-principles study

Xin Zhang(张鑫), Ruge Quhe(屈贺如歌), and Ming Lei(雷鸣)
Citation: Chin. Phys. B, 2022, 31 (**4**): 046401. DOI: 10.1088/1674-1056/ac3987
Journal homepage: http://cpb.iphy.ac.cn; http://iopscience.iop.org/cpb

What follows is a list of articles you may be interested in

Metal substrates-induced phase transformation of monolayer transition metal dichalcogenides for hydrogen evolution catalysis

Zhe Wang(王喆) and Wenguang Zhu(朱文光)
Chin. Phys. B, 2021, 30 (**11**): 116401. DOI: 10.1088/1674-1056/abfbd1

Novel structures and mechanical properties of Zr_2N: *Ab initio* description under high pressures

Minru Wen(文敏儒), Xing Xie(谢兴), Zhixun Xie(谢植勋), Huafeng Dong(董华锋), Xin Zhang(张欣), Fugen Wu(吴福根), and Chong-Yu Wang(王崇愚)
Chin. Phys. B, 2021, 30 (**1**): 016403. DOI: 10.1088/1674-1056/abb220

A high-pressure study of Cr_3C_2 by XRD and DFT

Lun Xiong(熊伦), Qiang Li(李强), Cheng-Fu Yang(杨成福), Qing-Shuang Xie(谢清爽), Jun-Ran Zhang(张俊然)
Chin. Phys. B, 2020, 29 (**8**): 086401. DOI: 10.1088/1674-1056/ab8c3d

Surface stabilized cubic phase of $CsPbI_3$ and $CsPbBr_3$ at room temperature

Feng Yang(杨凤), Cong Wang(王聪), Yuhao Pan(潘宇浩), Xieyu Zhou(周谐宇), Xianghua Kong(孔祥华), Wei Ji(季威)
Chin. Phys. B, 2019, 28 (**5**): 056402. DOI: 10.1088/1674-1056/28/5/056402

Compression behavior and spectroscopic properties of insensitive explosive 1,3,5-triamino-2,4,6-trinitrobenzene from dispersion-corrected density functional theory

Yan Su(苏艳), Junyu Fan(范俊宇), Zhaoyang Zheng(郑朝阳), Jijun Zhao(赵纪军), Huajie Song(宋华杰)
Chin. Phys. B, 2018, 27 (**5**): 056401. DOI: 10.1088/1674-1056/27/5/056401

Insights into the adsorption of water and oxygen on the cubic $CsPbBr_3$ surfaces: A first-principles study

Xin Zhang(张鑫)[1,2], Ruge Quhe(屈贺如歌)[1,†], and Ming Lei(雷鸣)[1,‡]

[1] *State Key Laboratory of Information Photonics and Optical Communications and School of Science, Beijing University of Posts and Telecommunications, Beijing* 100876, *China*

[2] *College of Aeronautical Engineering, Binzhou University, Binzhou* 256603, *China*

(Received 27 July 2021; revised manuscript received 11 November 2021; accepted manuscript online 15 November 2021)

The degradation mechanism of the all-inorganic perovskite solar cells in the ambient environment remains unclear. In this paper, water and oxygen molecule adsorptions on the all-inorganic perovskite ($CsPbBr_3$) surface are studied by density-functional theory calculations. In terms of the adsorption energy, the water molecules are more susceptible than the oxygen molecules to be adsorbed on the $CsPbBr_3$ surface. The water molecules can be adsorbed on both the CsBr- and PbBr-terminated surfaces, but the oxygen molecules tend to be selectively adsorbed on the CsBr-terminated surface instead of the PbBr-terminated one due to the significant adsorption energy difference. While the adsorbed water molecules only contribute deep states, the oxygen molecules introduce interfacial states inside the bandgap of the perovskite, which would significantly impact the chemical and transport properties of the perovskite. Therefore, special attention should be paid to reduce the oxygen concentration in the environment during the device fabrication process so as to improve the stability and performance of the $CsPbBr_3$-based devices.

Keywords: all-inorganic perovskite, structural and electronic properties, molecule adsorption, density functional theory

PACS: 64.70.Nd, 71.15.Mb, 73.61.Le **DOI:** 10.1088/1674-1056/ac3987

1. Introduction

Hybrid organic–inorganic perovskites (HOIPs) such as $MAPbI_3$ have emerged as a revolutionary class of materials in the fields of electronics, photovoltaics, and optoelectronics,[1] due to their unique features, such as small and adjustable bandgaps,[2] ambipolar charge transport properties,[3,4] limited charge recombination,[5–7] and the low-cost of production.[8–11] The structural formula of perovskites (ABX_3) is identified with a small organic ion occupies A-site, a divalent metallic atom occupies B site, and halogens are on the X sites. In just a few years, the photoelectric conversion efficiency of perovskite solar cells has increased from 3.81% to 25.2%.[10–12] However, the thermal stability issue of HOIPs under ultraviolet light illumination,[13,14] in a moisture environment,[15] or at high temperatures[16] is still a challenge to the whole community. The pure inorganic alternative, like $CsPbBr_3$, has been found to possess better stability. In the inorganic perovskite, inorganic ions replace the organic components of the hybrid perovskite, and the reaction path that the organic groups participate in is lost. Therefore, the chemical stability of the all-inorganic perovskite to oxygen is significantly improved from the aspect of degradation.[17] Moreover, $CsPbBr_3$ is expected to keep most of the good properties of the HOIPs counterparts.[18–20] $CsPbBr_3$ has excellent luminescent properties, including extremely high quantum yield, narrow emission bandwidth without size distribution, and suppressed photoluminescence (PL) blinking.[21] $CsPbBr_3$ also exhibits remarkably high carrier mobility and considerable diffusion length.[22] Besides, $CsPbBr_3$ can be synthesized in various structures such as quantum dots, nanocubes, nanowires, nanoplates, and even two-dimensional (2D) layers with controllable sizes.[23] This allows one to modulate the quantum confinement effect in the nanostructures to achieve desired emitting wavelength. All these features make $CsPbBr_3$ a very promising candidate for future optoelectronic and photovoltaic applications.

The adsorption of water molecules on the surface of solid materials plays an essential role in changing the surface structure and affecting the surface's stability and reactivity.[24–31] Computational modeling predicts a quite strong interaction between the $MAPbI_3$ inorganic scaffold and water molecules, which will presumably modify the perovskite crystal structure.[32] Recently, Aristidou *et al.*'s experiments have shown that the reaction of superoxide with the $CH_3NH_3^+$ cations can initiate the degradation of methylammonium lead trihalide perovskite photoactive layers.[33,34] In order to increase the stability of such materials, recent researches are devoted to protecting the perovskite layer from water-induced degradation processes.[22,35–37] In addition to the stability issue, previous experimental studies have shown that the efficiency of solar cells dropped when the cells were exposed to humid environment.[21–24] Similar to the HOIPs counterparts,

†Corresponding author. E-mail: quheruge@bupt.edu.cn
‡Corresponding author. E-mail: mlei@bupt.edu.cn

© 2022 Chinese Physical Society and IOP Publishing Ltd

understanding the interaction between the all-inorganic perovskite $CsPbBr_3$ surface and H_2O or O_2 molecules is a critical issue in developing commercially viable devices.

In this study, we investigate the adsorption of water and oxygen molecules on the cubic $CsPbBr_3$ surfaces on an atomic scale by using the first-principles calculations. Our calculation results suggest that both the PbBr-terminated and the CsBr-terminated surfaces of cubic $CsPbBr_3$ can strongly attract water molecules. The oxygen molecules tend to be adsorbed on the CsBr-terminated surface but not on the PbBr-terminated surface. We also found that the adsorption of water molecules on the two surfaces has little effect on the low-energy band structure of the cubic $CsPbBr_3$ surfaces, while the adsorption of oxygen molecules introduces interfacial states inside the bandgap of $CsPbBr_3$.

2. Method

The density-functional theory (DFT) calculations were carried out within the Vienna *ab initio* simulation package (VASP).[38] The exchange–correlation between electrons was described by the generalized gradient approximation (GGA) in the Perdew–Burke–Ernzerhof (PBE) form.[39,40] The interactions in chemical systems are mainly divided into strong interaction and weak interaction. The latter is usually an order of magnitude weaker than the former.[41] The van der Waals force is a kind of weak interaction. In this paper, we mainly studied molecular adsorption. The adsorption of water and oxygen molecules on the surface of $CsPbBr_3$ is mainly physical adsorption. The van der Waals corrections have also been included when studying similar systems, such as the adsorption of water and oxygen, as well as their coadsorption on tetragonal $CH_3NH_3PbI_3$ (001) surfaces,[30] and the heterogeneous interface between water and the prototypical $MAPbI_3$ perovskite.[31] So the PBE functional with optB86b-vdW[42] correction was adopted in all the calculations to yield more reliable results in the view of water and oxygen molecules involved in the surface calculations. A cutoff energy of 520 eV was chosen for the plane-wave basis set in all calculations. The relaxation of geometry optimization was continued until the residual force was less than 0.01 eV/Å, and the total energy was lower than 1×10^{-3} eV per atom. $3\times3\times1$ and $17\times17\times2$ Monkhorst–Pack k-point meshes were used for the geometry optimizations and static electronic structure calculations, respectively.

3. Results and discussion

3.1. Structural properties

It is well known that the perovskites undergo a series of phase transitions from cubic to tetragonal and to orthorhombic phases upon cooling.[43] The cubic (Pm-3m) phase of $CsPbBr_3$ is the most stable phase at high temperature (130 °C). In the current study, we focus on the cubic phase. The structure is octahedral with Pb at the center, and six halogens Cs exist at the corner of the cubic. The relaxed lattice parameter 6.01 Å is in good agreement with previous data by experiments and other calculations.[3,44–47]

Following the obtained geometric structure of the bulk cubic $CsPbBr_3$, the slab models representing the surfaces of $CsPbBr_3$ were established based on the optimized lattice parameters. The PbBr-terminated surface of the cubic $CsPbBr_3$ (Figs. 1(a) and 1(c)) was modeled by a slab supercell with 5 atomic layers, including 3 $PbBr_2$ layers and 2 CsBr layers. The CsBr-terminated surface (Figs. 1(b) and 1(d)) was modeled by a slab supercell with 6 atomic layers, including 3 danPbBr$_2$ layers and 3 CsBr layers. The atomic layers of both slabs were completely relaxed during the geometry optimization.

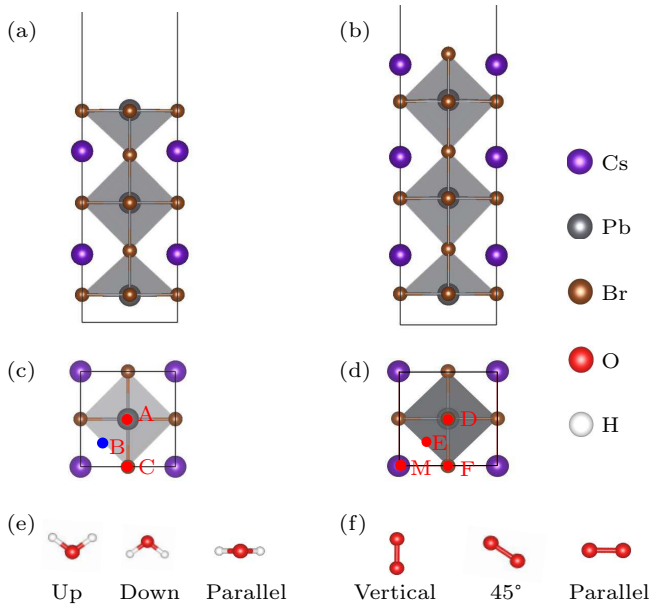


Fig. 1. (a)–(d) Side and top views of the PbBr- and CsBr-terminated $CsPbBr_3$ surfaces. The studied adsorption sites on the PbBr-terminated (sites A, B, and C) and the CsBr-terminated surfaces (sites D, E, F, and M) are labeled on panels (c) and (d), respectively. Different initial orientations of (e) water and (f) oxygen molecules on the specific sites.

According to the symmetry of the systems, the initial sites where the water and oxygen molecules placed are depicted in Figs. 1(c) and 1(d). The initial symmetrical sites on the PbBr-terminated surface include the top of the Pb atom (position A), the hollow position of the surface (position B), and the top of the I atom (position C). On the CsBr-terminated surface, the initial symmetrical positions include the top of the Br atom (position D), the hollow position of the surface (position E), the boundary midpoint (position F), and the top of the Cs atom (position M). Different initial orientations of the molecules on the specific position have been considered, including up, down, and parallel for the water molecules (Fig. 1(e)) and vertical, 45°, and parallel for the oxygen molecules (Fig. 1(f)). For water molecules, "up" means that the two hydrogen atoms

point to the top of the PbBr- and CsBr-terminated surfaces, "down" means that the hydrogen atoms point to the surfaces, and "parallel" means that the hydrogen-oxygen bond of the water molecule is basically parallel to the surfaces. Similarly, "vertical" means that the bond of the oxygen molecule is perpendicular to the surfaces, "45°" means that the angle between the oxygen–oxygen bond and the plane is about 45°, "parallel" means that the bond is approximately parallel to the surfaces.

To calculate the adsorption energy, one has to figure out the most stable adsorption configuration and the corresponding total energy of the system. This information provides a reference for future studies on the degradation mechanism of $CsPbBr_3$. As shown in the previous pioneer works by Liu and Mosconi,[31,48] the degradation mechanism of perovskite can be theoretically studied by either nudged elastic band or molecular dynamics techniques. Both two works studied the most stable adsorption configuration before degradation reaction. In the former, the energy difference between the transition state and the most stable adsorption state is calculated when determining the diffusion barrier. In the latter, the stable configuration could be applied as the starting point for a benchmark.

The adsorption energy E_{ads} of the molecule on the surface was calculated by

$$E_{ads} = E_{molecule/slab} - E_{slab} - E_{molecule}, \quad (1)$$

where $E_{molecule/slab}$, E_{slab}, and $E_{molecule}$ are the relaxed total energies of the adsorption system, pure slab model before adsorption molecules, and the free molecule in a vacuum, respectively.

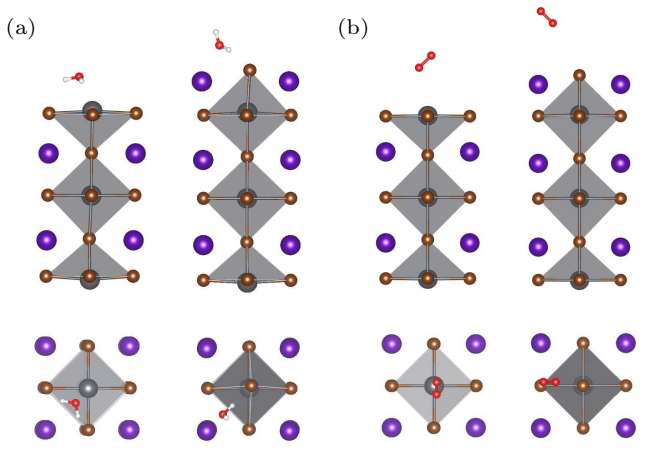


Fig. 2. Side and top views of the most stable structures of (a) H_2O- and (b) O_2-adsorbed $CsPbBr_3$ surfaces with PbBr-terminations and CsBr-terminations.

The adsorption of water molecules on the surface of solid materials plays an important role in changing the surface structure and affecting the stability and reactivity of the surface. In order to find out their stable adsorption sites, the adsorption of a single water molecule on surfaces was first investigated. Figure 2 shows the relaxation structures of water and oxygen molecules on the PbBr-terminated and CsBr-terminated surfaces. On the PbBr-terminated surface, the water molecule moves to site B (exists in parallel) during relaxation no matter which site is placed initially. On the CsBr-terminated surface, the water molecule moves to site E during relaxation when the water molecule was initially placed at site D and site E. The water molecule remains in the initial position during a relaxation for initial site F and site M. As a strong oxidant and one of the main constituents in air, the oxygen molecule is inevitable to interact with the surface of $CsPbBr_3$ when exposed to air. The geometric structures of the oxygen molecule at all the seven initial sites show that the orientation of the adsorbed oxygen molecule stays almost 45° at the initial sites during relaxation.

Table 1. Calculated adsorption energies (E_{ads}) and bandgaps (E_g) of H_2O- or O_2-adsorbed $CsPbBr_3$ surface. m_e and m_h are the electron and hole effective masses of H_2O- and O_2-adsorbed $CsPbBr_3$ surfaces. Q is the averaged Bader charge transferred from the $CsPbBr_3$ surface to the adsorbed molecules.

		PbBr-terminated surface			CsBr-terminated surface			
	Initial site	A	B	C	D	E	F	M
H_2O	Stable site	B	B	B	Near E	E	F	M
	E_{ads} (eV)	−0.51	−0.51	−0.51	−0.62	−0.59	−0.08	−0.53
	E_g (eV)	2.21	2.21	2.21	2.09	2.11	2.12	2.00
	m_e (m_0)	0.577	0.567	0.558	0.512	0.587	0.512	0.503
	m_h (m_0)	0.152	0.152	0.152	0.230	0.229	0.217	0.225
	Q (e)		−0.020		0.039			
	Stable site	A	B	C	D	E	F	M
O_2	E_{ads} (eV)	−0.13	0.02	0.05	−0.08	−0.32	−0.42	−0.23
	E_g (eV)	1.92	2.23	2.20	2.10	1.94	1.30	1.95
	m_e (m_0)	0.516	0.391	0.396	0.512	0.536	0.532	0.527
	m_h (m_0)	0.201	0.236	0.232	0.236	0.262	0.261	0.241
	Q (e)	0.143					0.207	

The adsorption energies of the water molecule and oxygen molecule on surfaces of cubic $CsPbBr_3$ are tabulated in Table 1 and Fig. 3, respectively. It is clearly shown that the water molecule is attractive to both the PbBr-terminated and CsBr-terminated surfaces. The adsorption energies of the water molecules initially on the three symmetry sites (A, B, and C) of the PbBr-terminated surface are basically the same. We also find from Fig. 3(a) that among four symmetry sites of D, E, F, and M, when the initial configuration of the water molecule on site E is down, the optimized structure has the smallest adsorption energy. The adsorption energy of water molecule on the symmetry site F is relatively small. The preferred adsorption sites for water molecules are the hollow site (site B) on the PbBr-terminated surface and site E on the CsBr-terminated surface. Figure 3(b) shows the adsorption energies of oxygen molecules at initial sites on the PbBr-terminated and CsBr-terminated surfaces. The adsorption energy of the PbBr-terminated surface for oxygen molecules is close to zero, and the initial configuration of the F point of the CsBr plane at 45° is most conducive to the adsorption of oxygen molecules. The

preferred adsorption sites for oxygen molecules are site A on the PbBr-terminated surface and site F on the CsBr-terminated surface, which are different from the water molecules.

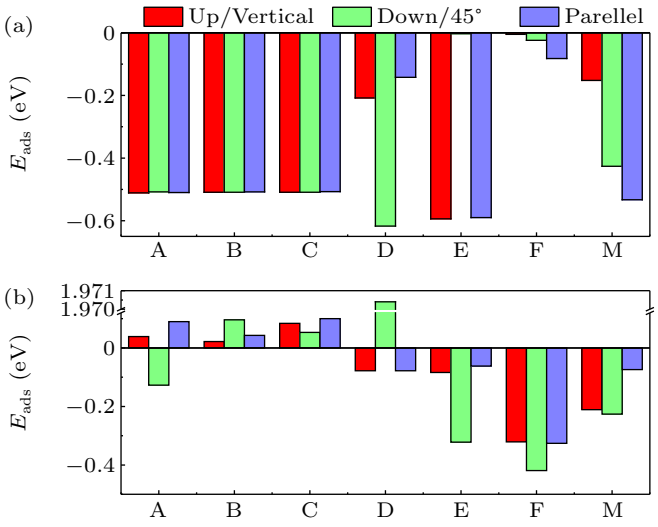


Fig. 3. Adsorption energies of (a) water and (b) oxygen molecules on sites A, B, and C of the PbBr-terminated surface and sites D, E, F, and M of the CsBr-terminated surface.

On the PbBr-terminated surface, the adsorption energy of oxygen molecules (−0.13 eV) is much larger than that of water molecules (−0.51 eV). Such an energy distinction means the tendency of the PbBr-terminated surface of cubic $CsPbBr_3$ to adsorb water molecules rather than the oxygen molecules. On the CsBr-terminated surface, the adsorption energy of oxygen molecules (−0.42 eV) is comparable to that of water molecules (−0.62 eV). And thus both oxygen and water molecules are preferred to be adsorbed on the CsBr-terminated surface of cubic $CsPbBr_3$. Here, we also found a metastable configuration in which water molecules are adsorbed at site E with an adsorption energy of −0.59 eV.

To check the uncertainty of adsorption energy, we further calculated and compared the adsorption energies of the most stable structure through different methods (GGA-PBE, GGA-PW91, and LDA-CA-PZ).[49] As shown in Table 2, the differences range from 0.031 eV to 0.054 eV which is one order of magnitude smaller than the adsorption energy and can be safely neglected. The uncertainty of the adsorption energy is estimated to be around 7.4%–8.75%. The adsorption energy of water and oxygen molecules obtained by LDA-CA-PZ and GGA-PW91 are almost the same. The water molecule adsorption results obtained by LDA-CA-PZ and GGA-PW91 are slightly larger than GGA-PBE, while the oxygen molecule adsorption results are slightly smaller than GGA-PBE. It can be seen that the adsorption energy has minor sensitivity to different functions and basis sets.

The temperature might play a key role in the degradation/interaction between molecules and perovskite surfaces.[31] Therefore, it is suggested to systematically investigate the dynamics under different temperatures by means of molecular dynamics when theoretically study the degradation and reaction mechanisms of $CsPbBr_3$ in the future.

Table 2. Comparison of results calculated at the GGA-PBE, GGA-PW91, and LDA-CA-PZ levels. E_{ads} is the adsorption energies of H_2O- or O_2-adsorbed $CsPbBr_3$ surface.

		GGA-PBE	GGA-pw91	LDA-CA-PZ
E_{ads} (eV)	H_2O	−0.617	−0.563	−0.570
	O_2	−0.419	−0.452	−0.450

3.2. Electronic properties

Comparing the adsorption energies of all initial symmetrical sites, the most stable adsorption site for water molecules is site E on the CsBr-terminated surface, and that for oxygen molecules is site F on the CsBr-terminated surface. The electronic band structures and projected state density (PDOS) of the bulk cubic $CsPbBr_3$, the PbBr-terminated and the CsBr-terminated surfaces are shown in Fig. 4, respectively. The band structures indicate a semiconducting feature with a direct bandgap of all three structures. The conduction band minimum (CBM) and the valence band maximum (VBM) of the bulk cubic structure are located at the R point, while the CBM and VBM of the two surfaces are located at the S point. The PbBr-terminated and the CsBr-terminated surfaces show slightly larger bandgaps (2.23 eV and 2.13 eV) than the bulk cubic structure (1.73 eV). It is interesting to note that the contribution from the surface atoms of the PbBr-terminated surface spread among all the energy levels from −4 eV to 4 eV. By contrast, the contribution from the surface atoms of the CsBr-terminated surface mainly distributes in the energy level about −2 eV.

The electronic band structures and the projected state density (PDOS) of water adsorbed surfaces are shown in Fig. 5. The bandgaps show almost no change after the adsorption of water molecules on the PbBr-terminated and the CsBr-terminated surfaces. No matter the water molecules are adsorbed on the PbBr-terminated or the CsBr-terminated surface, the contribution from H atoms is found little in the energy level from −4 eV to 4 eV. Therefore, the projection of the H atom is almost invisible on the projected state density (PDOS). The contribution from the adsorbed O atoms on the PbBr-terminated surface distributes in the energy level about −4 eV to −2 eV while they are localized in the energy level about −2 eV on the CsBr-surface. On the PbBr-terminated surface, the adsorbed O atoms' contribution in the large energy range as well as the PDOS overlap between Pb and O atoms indicate the strong Pb–O bonding characteristics, enhancing the adsorption capacity of Pb atoms.

The band structures and PDOS of the most stable oxygen molecules adsorbed PbBr- and CsBr-terminated surfaces are shown in Fig. 6. Unlike the case of H_2O adsorption, significant contributions of the O_2 are found inside the bandgap of

$CsPbBr_3$ for both PbBr- and CsBr-terminated surfaces. These interfacial states are expected to strongly affect the behavior of photo-induced carriers and carrier mobilities of $CsPbBr_3$.

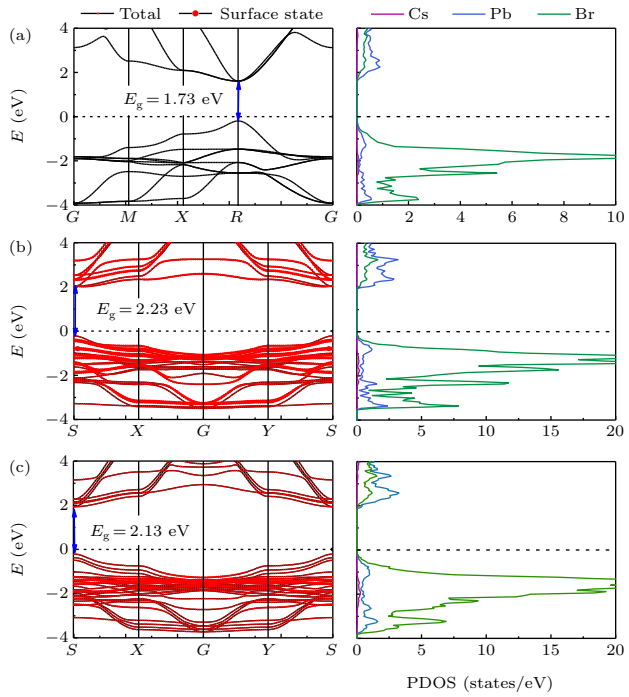


Fig. 4. Band structures and partial density of states (PDOS): (a) bulk $CsPbBr_3$, (b) PbBr-terminated surface, and (c) CsBr-terminated surface. The red dots represent projection weights of surface atoms. The Fermi level is set at zero.

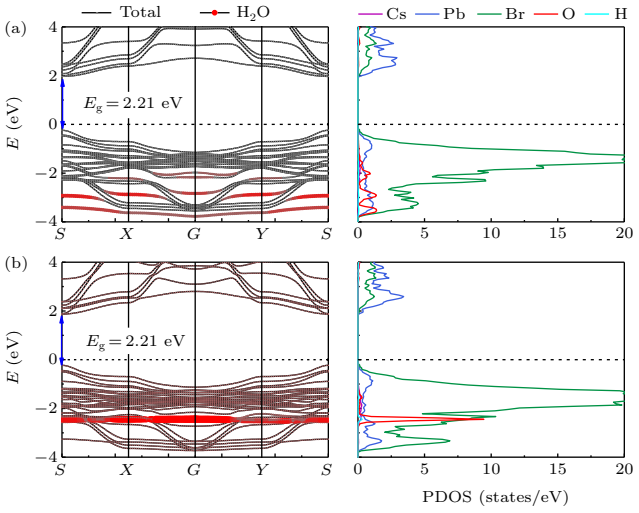


Fig. 5. Band structures and partial density of states (PDOS) of H_2O-adsorbed (a) PbBr-terminated surface and (b) CsBr-terminated surface. H_2O is located at site B in panel (a) and site D in panel (b). The red dots represent projection weights of the adsorbed water molecule. The Fermi level is set at zero.

In Table 1, the effective masses are presented, which are obtained by fitting the energy bands with parabolic curves at the valence band maximum (VBM) and conduction band minimum (CBM). When the water and oxygen molecules adsorb to the PbBr-terminated surface, the effective mass of electrons ranges from $0.391m_0$ to $0.577m_0$ while the hole effective mass is only $0.152m_0$ to $0.236m_0$. On the CsBr-terminated surface, such a difference between the electron and hole effective mass is also found: the electron effective mass ranges from $0.503m_0$ to $0.587m_0$ while the hole effective mass is $0.217m_0$ to $0.236m_0$. Among them, we noticed the calculated effective masses for the three similar structures (optimization results of water molecules on the PbBr-terminated surface) are quite similar. The slight difference is attributed to the small structure difference. The fitting error of the effective mass is estimated from 1.47% to 3.57%.

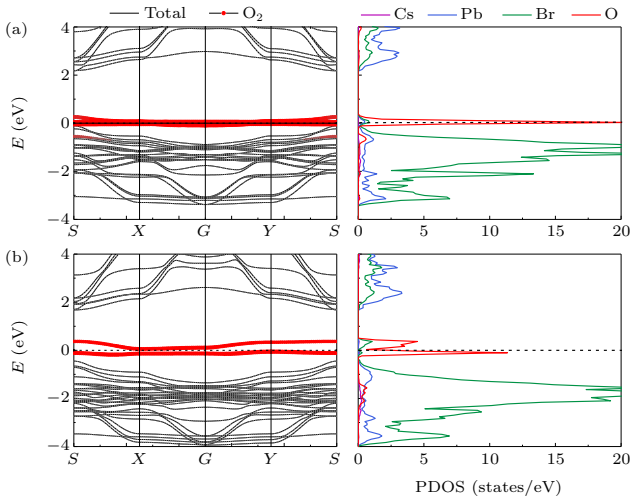


Fig. 6. Band structures and partial density of states (PDOS) of O_2-adsorbed (a) PbBr-terminated surface and (b) CsBr-terminated surface calculated by PBE. O_2 is located at site A in panel (a) and site F in panel (b). The red dots represent projection weights of the adsorbed oxygen molecule. The Fermi level is set at zero.

To analyze the charge transfer between the adsorbed molecules and terminated surfaces, we performed the Bader charge analysis. In Table 1, Q is defined as the number of electrons transferred from the PbBr- and CsBr-terminated surfaces to the water or oxygen molecules per supercell. On both the PbBr- and CsBr-terminated surfaces, the adsorbed oxygen molecules obtain more than $0.1e$ from the surfaces. The water molecules obtain electrons ($0.04e$) from the CsBr-terminated surface. When the water molecules are adsorbed on the PbBr-terminated surface, neglectable charge transfer less than $0.02e$ from water to the surface is found.

In addition to the lowest energy state, other metastable adsorption configurations may also exist. Therefore, we also studied the electronic properties of various types of different adsorption configurations. For the details of the band structures and PDOS, please refer to the supporting information. The electronic structures of the metastable configurations are found to be quite similar to the stable ones for both H_2O and O_2 adsorptions. In supporting information, Figs. S1 and S2, the band structures of the typical metastable configuration with H_2O and O_2 adsorption are presented. Like the cases of the most stable configuration, a small contribution from the adsorbed H_2O molecules but a significant one from the O_2 molecules is found in the low-energy region. Therefore, we believe the adverse impact on the transport proper-

ties of $CsPbBr_3$ originating from the interfacial states inside the bandgap is common for the O_2 adsorption on the cubic $CsPbBr_3$ surfaces. A slight difference between the metastable and stable ones is that the states of the O atoms in the adsorbed H_2O distribute around the energy level of -3 eV while they are around -2 eV in the most stable configuration, when H_2O is adsorbed on the CsBr-terminated surfaces.

This work studied the $CsPbBr_3$ system only. Although it is hard to say whether the findings are valid for other all-inorganic perovskites, some interesting results are found when carefully comparing $CsPbBr_3$ with other perovskites studied by previous works: First, Pb–O interaction plays an important role in stabilizing the H_2O adsorbed PbBr-terminated $CsPbBr_3$ surface. A similar phenomenon is found in the H_2O adsorbed PbI_2-terminated $CH_3NH_3PbI_3$ surface.[30] Second, on the $CsPbBr_3$ surface, the contributions of O_2 molecules are close to the Fermi level. A similar conclusion is reported in the O_2-adsorbed $CH_3NH_3PbI_3$ surface.[30] The calculations results suggest that the adsorbed oxygen molecule introduces empty states near the Fermi level, which would facilitate the charge transfer between oxygen molecule and surface. Considering the similar properties of different all-inorganic perovskites, it is worthy to check if these two findings are valid too.

Recently, we have seen rapid progress in the growth and device fabrication of bulk $CsPbBr_3$. However, since the toxicity of Pb poses a threat to the environment, developing lead-free perovskites,[50–53] such as Sn-, Ge-, Sb-, and Bi-based ones, is a promising research direction. Moreover, the change of dimensionality of metal hybrid perovskites from bulk to low-dimension is reported to enhance the phase and environmental stability.[48] Therefore, more work should be done to clarify how the composition and dimension variations affect the H_2O and O_2 adsorption behaviors of all-inorganic perovskites.

4. Conclusion

In conclusion, the structural and electronic properties of water and oxygen molecule adsorptions on the PbBr- and CsBr-terminated surfaces of cubic $CsPbBr_3$ have been investigated by means of density functional theory. It is found that both the PbBr- and CsBr-terminated surfaces can strongly attract water molecules. However, the adsorption results of oxygen molecules are different from those of water molecules. Due to the significant difference in adsorption energy, oxygen molecules tend to selectively adsorb on the CsBr-terminated surface rather than the PbBr-terminated surface. In the density of states, the contributions of the adsorbed H_2O molecules on both the CsBr- and PbBr-terminated surfaces are mainly at the deep energy level (-2 eV to -4 eV). On the contrary, the contributions of O_2 molecules are close to the Fermi level. Our study presents a thorough understanding of the interaction between the water or oxygen molecules and the all-inorganic perovskite $CsPbBr_3$ surface, and provides a reference for developing stable and high-performance devices based on $CsPbBr_3$ in the future.

Acknowledgments

Project supported by the Fundamental Research Funds for the Central Universities, and the National Natural Science Foundation of China (Grant Nos. 91964101 and 11905016), a Project of Shandong Provincial Higher Educational Science and Technology Program (Grant No. J18KB108), the Fund from the State Key Laboratory of Artificial Microstructure & Mesoscopic Physics, and the Fund of the State Key Laboratory of Information Photonics and Optical Communications (Beijing University of Posts and Telecommunications). We also thank the support from the High-performance Computing Platform of Peking University.

References

[1] Li Z, Klein T R, Kim D H, Yang M, Berry J J, Van Hes M F A M and Zhu K 2018 *Nat. Rev. Mater.* **3** 18017
[2] Lee M M, Teuscher J, Miyasaka T, Murakami T N and Snaith H J 2012 *Science* **338** 643
[3] Burschka J, Pellet N, Moon S J, Humphry-Baker R, Gao P, Nazeeruddin M K and Gratzel M 2013 *Nature* **499** 316
[4] Zhou H P, Chen Q, Li G, Luo S, Song T B, Duan H S, Hong Z R, You J B, Liu Y S and Yang Y 2014 *Science* **345** 542
[5] Jeon N J, Noh J H, Yang W S, Kim Y C, Ryu S, Seo J and Seok S I 2015 *Nature* **517** 476
[6] MØller C K 1958 *Nature* **182** 1436
[7] Tanaka K T, Ban T, Kondo T, Uchida K and Miura N 2003 *Solid State Commun.* **127** 619
[8] Stranks S D E, Grancini G, Menelaou C, Alcocer M J P, Leijtens T, Herz L M, Petrozza A and Snaith H J 2013 *Science* **342** 341
[9] Xing G M, Sun N, Sun S, Lim S S, Lam Y M, Grätzel M, Mhaisalkar S and Sum T C 2013 *Science* **342** 344
[10] Wehrenfennig C, Eperon G E, Johnston M B, Snaith H J and Herz L M 2014 *Adv. Mater.* **26** 1584
[11] Ponseca C S, Savenije Jr, Abdellah T J, Zheng M, Yartsev K, Pascher A, Harlang T, Chabera T, Pullerits P, Stepanov T, Wolf A and Sundstrom J P V 2014 *J. Am. Chem. Soc.* **136** 5189
[12] Kim J, Anita H B and Huang S J 2019 *Sol. RRL* **3** 1800302
[13] Li X, Wu Y, Zhang S, Cai Bi, Gu Y, Song J and Zeng H 2016 *Adv. Funct. Mater.* **26** 2435
[14] Wei J, Wang Q W, Huo J D, Gao F, Gan Z Y, Zhao Q and Li H B 2020 *Adv. Energy Mater.* **11** 2002326
[15] Protesescu L, Yakunin S, Bodnarchuk M I, Krieg F, Caputo R, Hendon C H, Yang R X, Walsh A and Kovalenko M V 2015 *Nano Lett.* **15** 3692
[16] Husin S A S, Muhammad F D, Che A C A, Ribut S H, Zulkifli M Z and Mahdi M A 2019 *Chin. Phys. B* **28** 84207
[17] Zhou Y and Zhao Y 2019 *Energy Environ. Sci.* **12** 1495
[18] Swarnkar A, Chulliyil R, Ravi V K, Irfanullah M, Chowdhury A and Nag A 2015 *Angew. Chem.* **54** 15424
[19] Yettapu G R, Talukdar D, Sarkar S, Swarnkar A, A Nag, Ghosh P and Mandal P 2016 *Nano Lett.* **16** 4838
[20] Yang F, Wang C, Pan Y, Zhou X, Kong X and Ji W 2019 *Chin. Phys. B* **28** 056402
[21] Niu G, Li W, Meng F, Wang L, Dong H and Qiu Y 2014 *J. Mater. Chem. A* **2** 705
[22] Yang J L, Siempelkamp B D, Liu D Y and Kelly T L 2015 *Acs Nano* **9** 1955
[23] Gratzel M 2014 *Nat. Mater.* **13** 838
[24] Leijtens T, Eperon G E, Pathak S, Abate A, Lee M M and Snaith H J 2013 *Nat. Commun.* **4** 2885

[25] Martinez-Gonzalez J A, English N J and Gowen A A 2021 *Mol. Simulat.* **47** 666
[26] Liu Y C, Chen J H, Li Y Q, Zhang J J and Kang D 2021 *Physicochem. Probl. Miner. Process.* **57** 121
[27] Lin Y T, Smith N J, Banerjee J, Agnello G, Manley R G, Walczak W J and Kim S H 2021 *J. Am. Ceram. Soc.* **104** 1568
[28] Li S Q, Chang Y, Zhang Z, Liu H S, Chen M D, Han Y, Gao J F and Zhao J J 2021 *J. Phys. Chem. C* **125** 667
[29] Zhang L H and Sit P H L 2015 *J. Phys. Chem. C* **119** 22370
[30] Hao W, Chen X and Li S 2016 *J. Phys. Chem. C* **120** 28448
[31] Mosconi E, Azpiroz J M and De Angelis F 2015 *Chem. Mater.* **27** 4885
[32] Dong X, Fang X, Lv M, Lin B, Zhang S, Ding J and Yuan N 2015 *J. Mater. Chem. A* **3** 5360
[33] Aristidou N, Sanchez-Molina I, Chotchuangchutchaval T, Brown M, Martinez L, Rath T and Haque S A 2015 *Angew. Chem.* **54** 8208
[34] Aristidou N, Haque S, Eames C, Sanchezmolina I, Bu X, Kosco J, Saiful Islam M and Haque S 2017 *Nat. Commun.* **8** 15218
[35] Leguy A, Hu Y, Campoy-Quiles M, Alonso M I, Weber O J, Azarhoosh P, Schilfgaarde M, Weller M T, Bein T, Nelson J, Docampo P and Barnes P R F 2015 *Chem. Mater.* **27** 3397
[36] Han Y, Meyer S, Dkhissi Y, Weber K, Pringle J M, Bach U, Spiccia L and Cheng Y B 2015 *J. Mater. Chem. A* **3** 8139
[37] Chen S, Solanki A, Pan J S and Sum T C 2019 *Coatings* **9** 535
[38] Vackar J, Simunek A and Podloucky R 1996 *Phys. Rev. B* **53** 7727
[39] Kresse G and Furthmuller J 1996 *Phys. Rev. B* **54** 11169
[40] Perdew J P, Burke K and Ernzerhof M 1996 *Phys. Rev. Lett.* **77** 3865
[41] Emamian S, Lu T, Kruse H and Emamian H 2019 *J. Comput. Chem.* **40** 2868
[42] Michaelides A, Ranea V A, de Andres P L and King D A 2003 *Phys. Rev. Lett.* **90** 216102
[43] Weerd C D, Lin J H, Gomez L, Fujiwara Y, Suenaga K and Gregorkiewicz Tom 2017 *J. Phys. Chem. C* **121** 19490
[44] Baikie T, Fang Y, Kadro J M, Schreyer M, Wei F, Mhaisalkar S G, Graetzel M and White T J 2013 *J. Mater. Chem. A* **1** 5628
[45] Ye Y, Run X, Tao X H, Feng H, Fei X and Lin J W 2015 *Chin. Phys. B* **24** 116302
[46] Lang L, Yang J H, Liu H R, Xiang H J and Gong X G 2014 *Phys. Lett. A* **378** 290
[47] Ahmad M, Rehman G, Ali L, Shafip M, Iqbal R, Ahmad R, Khan T, Jalali-Asadabadi S, Maqbool M and Ahmad I 2017 *J. Alloys Compd.* **705** 828
[48] Tong C J, Geng W, Tang Z K, Yan C Y and Fan S L 2015 *J. Phys. Chem. L* **6** 3289
[49] Shen Y, Lu P F, Yu Z Y, Zhao L, Ye H, Liu Y M and Yuan G F 2011 *Commun. Theor. Phys.* **55** 693
[50] Yang J X, Zhang P, Wang J P and Wei S H 2020 *Chin. Phys. B* **29** 108401
[51] Li Z Q, Li Z L, Shi Z F and Fang X S 2020 *Adv. Funct. Mater.* **30** 2002634
[52] Lei J H, Tang Q, He J and Cai M Q 2021 *Chin. Phys. B* **30** 038102
[53] Wang H P, Li S Y, Liu X Y, Shi Z F, Fang X S and He J H 2021 *Adv. Materials* **33** 2003309